Journal of Alloys and Compounds 489 (2010) 523–529

Contents lists available at ScienceDirect

Journal of Alloys and Compounds

journal homepage: www.elsevier.com/locate/jallcom

Development of high DC-bias Mn–Zn ferrite working at frequency higher than 3 MHz

Yapi Liu [a,b,*], Shijin He [b]

[a] Department of Material Science and Engineering, China Jiliang University, Hangzhou 310018, China
[b] Workstation for Post-Doctor Scientific Research, DMEGC, Dongyang 322118, China

ARTICLE INFO

Article history:
Received 28 May 2009
Received in revised form
17 September 2009
Accepted 17 September 2009
Available online 25 September 2009

Keywords:
Mn–Zn ferrite
DC-bias magnetic field
High frequency
Low loss
Power ferrite
Cutoff frequency

ABSTRACT

Modern high-frequency electronic technology demands Mn–Zn soft ferrite for high DC-bias and low power loss applications. In this study, DMR50B ferrite material with a very attractive DC-bias property and with a lower power loss at high frequency up to 3 MHz was developed employing a conventional ceramic powder processing technique based on our previous study of DMR50 material, indicating its magnetic properties can be further improved by microstructure homogeneity. The core loss is around 200 kW/m^3 at 3 MHz, 10 mT and 100 °C, and only around 20 kW/m^3 at 700 kHz, 30 mT and 100 °C; its cutoff frequency f_r is ~4 MHz and its incremental permeability μ_Δ remains constant until H_{DC} = 100 A/m. Furthermore, the electromagnetic characteristics and the microstructure of this new DMR50B material are also discussed.

1. Introduction

The performance of the soft magnetic Mn–Zn power ferrite core for high-frequency switching power supplies is determined by the ability for the core to handle large signal or to realize power transfer at high frequencies and high induction levels at the expense of low energy loss. Due to the demands for more compact, lighter and thinner electronic devices and equipments, there has been a critical need for Mn–Zn ferrites with even higher permeability and even lower power loss at higher frequency (up to a few MHz) [1,2]. In addition, in many applications when large amount of DC must be tolerated, such as in ADSL applications where the electronic circuit may carry DC current of 100 mA in average, the core material also must exhibit a high incremental permeability (μ_Δ) (also known as reversible permeability μ_{rev} when AC magnetic field is very small) at a higher DC-bias magnetic field H_{DC} (the so-called DC-bias behavior) [2]. In the telecommunication industry, the core material also has to be very stable under environmental or operating conditions since the linearity of μ with a DC-bias is needed. This behavior can be achieved by high saturation of the ferrite material [2]. Therefore, the high DC-bias property of the cores is also the main concern for high-frequency applications except for lower power loss regarding soft power ferrite applications.

As a basic approach for development of the low loss materials, research and analysis have been conducted to unravel the mechanisms of loss generation in Mn–Zn ferrites [1,3,4]. The energy loss phenomena in these materials are insufficiently assessed since various physical mechanisms responsible for these losses are effective at different frequency ranges. Theoretically, the power loss in ferrites is generally split up into three contributions with quite different physical origins [1,5–9]:

$$P_C = P_h + P_e + P_r = K_H B^3 f + \frac{K_E B^2 f^2}{\rho} + P_r \quad (1)$$

where P_C is the total power loss, P_h, P_e and P_r are the hysteresis loss, eddy current loss and residual loss, respectively, K_H and K_E are constants, B is the magnetic flux density, f is the frequency and ρ is the electrical resistivity. Apart from the contributions to P_e, the understanding of ferrite dissipation is mainly phenomenological [1,9]. The justification for this subdivision resides partially in differences in the frequency response of each loss contribution.

The proportions of these components in the total loss vary widely according to measurement conditions such as frequency f and magnetic flux density B. P_h denotes the loss due to the hysteretic nature of the magnetization reversal. This loss contribution is basically determined by the energy dissipation of a static hysteresis loss loop multiplied by frequency (f) by which the magnetization

* Corresponding author at: Department of Material Science and Engineering, China Jiliang University, Xiasha Higher Education Zoo, Hangzhou 310018, China. Tel.: +86 57186835743; fax: +86 57188082785.
E-mail addresses: yapiliu@gmail.com, yapiliu@cjlu.edu.cn (Y.P. Liu).

0925-8388/$ – see front matter © 2009 Elsevier B.V. All rights reserved.
doi:10.1016/j.jallcom.2009.09.099

is reversed. The energy dissipation, which corresponds to a cycle of the hysteresis loop, is considered to be proportional to B^3 (as can be seen from Eq. (1)). At low frequencies P_h is dominant, and in order to reduce P_h, it is important to form uniform microstructure which is free from lattice defects and pores so as not to obstruct the movements of the magnetic domain walls.

P_e denotes the loss due to eddy currents induced by the alternating magnetic field and hence depends greatly on the electrical resistivity of the material. At high frequencies, the proportion of P_e increases, and the enlarged P_e can be reduced by increasing the resistance of the core. The electrical resistivity of Mn–Zn ferrite is expected to increase by raising the electrical resistivity of the spinel matrix and grain boundary, and also the reduction of grain size, which contributes to increase the possibility of intersection of the grain boundary with eddy current.

Finally, P_r denotes the residual loss whose physical origin is less well understood. It is found that P_r becomes dominant at high frequency, and plays an important role in reducing power loss in the MHz range [3,8,9]. P_r is associated with magnetic relaxations and resonances in MHz ranges in the ferrite [8]. Magnetic relaxations contributing to these losses are due to domain wall excitations by the driving AC magnetic field. Magnetic resonance may occur in two ways, viz., rotational resonance and domain wall resonance. It is reported that the core losses of ferrites in the MHz range are lowered with decreasing the grain size [9–11]. Although not understood sufficiently, the cause of this effect is supposed that any magnetic resonance would be suppressed. For example, the suppression of natural resonance can be considered. It is known that the domain of ferrites is subdivided and that the numbers of domain walls per volume increase with a decrease of the grain size [9–11]; therefore, the amplitude of vibration in each domain wall is reduced in the same maximum induction B_m. In other words, the switching frequency of the spin inside the domain wall is reduced. It is found that the lower P_r of the developed ferrite is presumably caused by the suppression of the natural resonance for the spin inside the domain wall at 1 MHz owing to low resonance frequency f_r [12]. We have found that the resonances that occurred in power ferrites at MHz range are rotational resonance, and the corresponding loss can be reduced by using fine grains [13].

As explained above, the means of reducing the three components of loss often contradict with each other, and accordingly it is necessary to identify which component of loss will become dominant under the intended operational conditions.

As far as we know, power ferrites ideally have their anisotropy compensation point (at which K_1 passes through zero) at the normally operating temperature of 80–100 °C for a transformer through selecting a proper Fe-excess composition and by adjusting the partial oxygen pressure of the sintering atmosphere [8,12]. Because the transformer core is usually operated at these intended working temperatures, the power losses P_{CV} of power ferrite materials should reach this minimum at that temperature, where P_{CV} is the total power loss per volume.

Recently, many efforts have been made to improve the magnetic property of Mn–Zn soft ferrite, including enhanced maximum induction B_m and reduced power loss P_{CV} at higher frequencies. Some are concentrated on the effects of doping additives [14–16] and substitution elements [17] on electromagnetic performance of Mn–Zn soft ferrite, as besides the basic composition and sintering process, additions and substituents can play an important role in determining the magnetization and other properties of Mn–Zn ferrite, and can also influence the microstructure, intrinsic property, atomic diffusion, sintering kinetics, and the loss of Mn–Zn ferrite significantly. Meanwhile, the loss mechanism is also analyzed [14].

The spinel ferrites are usually prepared by a ceramic process through pressing a prefired mixture of powders to obtain the required shape and then converting it into a magnetic ceramic component by sintering. The prefired powder in such a process is inhomogeneous in chemical composition and has a number of large-size particles with a non-uniform size distribution. Moreover, the prefired powder consists usually of many individual phases that react with each other to form the desired spinel phase during the final firing step [18]. In order to overcome the difficulties arising from the ceramic method and in order to prepare soft ferrites with excellent electromagnetic performance, in recent years, due to the rapid development of nanotechnology, several methods including combinatorial synthesis and high throughput screening method [19], mechanochemical processing [20,21], and numerous wet chemical methods including the co-precipitation method, the hydrothermal process, sol–gel synthesis, and the micro-emulsion approach, have been proposed to synthesize Mn–Zn ferrite nanoparticles [18, and references therein], but nanoparticles were rarely used to develop MnZn soft ferrite core further in these papers. Moreover, it is also found that the high-permeability and low power loss can be achieved using nanocrystalline ferrites in place of micro-magnetic ferrites [22].

In our previous study [13], low loss Mn–Zn ferrite DMR50 that can work at frequency higher than 3 MHz was developed. Its P_{CV}–T curves showed that P_{CV} strikingly increases and the minimum loss temperature T_{min} at which the power loss gets to its minimum value gradually decreases with increasing frequency, revealing that its relatively high P_r is a main cause of the frequency dependence of T_{min} in high frequency [7,13], which can be confirmed by later discussion.

Microstructure is, of course, another key parameter that dominates the electrical and magnetic properties of Mn–Zn ferrites. In-depth investigation of the microstructure of the old DMR50 ferrite material using SEM [13] showed that there exist many porosities in the grains and also at the grain boundary regions with exaggerated grain growth. The ferrite material thus presents poor microstructure homogeneity though the average diameter of the grain is about 2.55 μm, smaller than the single domain dimension needed for Mn–Zn ferrites [9–13]. The distributions of pores inside and outside the grains and of larger grains have great effects on the magnetic and electrical properties of ferrites as described above, suggesting that the material can be further optimized to improve its magnetic properties by a low r volume fraction of pores and homogeneous grains. In addition, since the DC-bias property of this material is not very attractive, the efforts have been exerted to improve their electromagnetic characteristics by controlling the size of grains and the distribution of small amounts of additives in the grain boundary region during the producing routine.

In this study, based on our previous work the process routine was further optimized. The chemical composition of main elements of Mn–Zn ferrite was further adjusted to improve its B_m. To improve its microstructure, optimized combinations of CaO, SiO_2 and other additives such as Nb_2O_5, ZrO_2 and TiO_2 were carefully adjusted. The size of the green powder, the green density of the cores, and sintering process including the heating and cooling rate were all carefully controlled to avoid exaggerated grain growth. As the sintering process, for example, sintering temperature, isothermal duration and sintering atmosphere will influence the microstructure. To achieve fine grains for reducing P_r, the growth of the grain is controlled by using low sintering temperature technique. Small grains can be realized by applying finer powders, enabling sintering at lower temperatures during shorter periods. Also applying sinter acids may lower the sintering temperature and thus yields small grains [8]. Because of their low melting points, these oxides melt at grain boundaries and initially act as a grain growth inhibitor.

As P_r is lowered by fine grains, P_h and P_e are also improved by total optimization of preparation conditions as will be seen later. Eventually, compared to recent reports on P_{CV} [13,14], a ferrite material DMR50B with a much lower loss in a wide high frequency

range up to 3 MHz was obtained with higher DC-bias property through a very well controlled preparation process. In addition, taking fully into account the mass production conditions of the company, a conventional ceramic powder processing technique was employed.

2. Experimental

The chemical composition of Mn–Zn ferrite is $Mn_{0.73}Zn_{0.12}Fe_{2.15}O_4$. Commercial Fe_2O_3 are carefully chosen in such that the SiO_2 and CaO doping levels used are similar to the impurity levels in it. The cores of toroidal shape with 25 mm in outer diameter, 15 mm in inner diameter, and 8 mm in height are produced employing a conventional ceramic processing technique, and the samples are sintered in carefully controlled oxygen partial pressure. The relation between the cooling temperature and oxygen partial pressure is maintained according to the following equation [3]:

$$\log P_{O_2} = -\frac{14,540}{T[K]} + a \quad (2)$$

where atmospheric parameter "a" is a constant value, which is 7.8 in our experiment. Detailed process of producing is described elsewhere [13].

Power losses were measured using an Iwatsu BH analyzer (SY8232). An RF Impedance/Material Analyzer (Agilent 4291B) was used to measure the magnetic spectrum and the temperature dependence properties of permeability. A Hewlett-Packard impedance analyzer (4284A Precision LCR Meter) was used to measure the DC-bias properties, and the DC magnetic properties of the samples were measured by a MATS-2000 Magnetic Material Automatic Meter. X-ray diffraction (XRD) measurements were carried out with an X-ray powder diffraction (Rigaku D/Max-3B). The crystalline phases were identified with the Bragg peaks indexed and the lattice parameter calculated. Images of microstructures were obtained by means of a scanning electron microscope (SEM) (Hitachi S-570).

3. Results and discussion

3.1. XRD

In Fig. 1 the XRD pattern of the DMR50B material is shown. The (h,k,l) values corresponding to the diffraction peaks are marked in the figure. XRD analysis clearly exhibits that almost all the observed diffraction peaks, the interplanar distances d, Miller indices (h,k,l) and relative intensities I/I_0 (where I_0 is the maximum intensity) of this material match well with the reflections of manganese ferrite reported in the standard card with no extra lines, revealing thereby the sample was well crystallized in the single phase cubic spinel structure during the sintering process as there were no unreacted constituents, no other phases and no crystal deformation presented in the sample. This fact shows that the producing process is well controlled and also is suitable. As far as we know, the lattice constant "a" of a spinel ferrite will change with the chemical composition. The lattice parameter "a" of the sintered sample of this material calculated from the diffraction peak is 8.4985(4) Å, almost the same as that of previous report (DMR50, which is 8.4975(2) Å [13]).

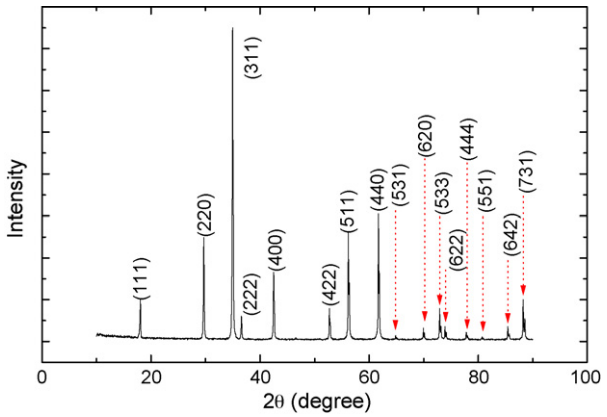

Fig. 1. XRD pattern of DMR50B material.

3.2. Power loss

A summary of the important magnetic properties for this new DMR50B material is given in Table 1, together with that of old DMR50. For comparison, 3F4 of Ferroxcube is also listed. As can be seen from Table 1, the overall power losses of this DMR50B material have been improved a lot compared to that of DMR50. The well controlled preparation process and the most optimum percentage of the sintering additives lead to sufficient densification while maintaining controlled grain growth, and it is under these conditions that the optimum magnetic performance of this new DMR50B material is achieved during wide frequency range.

It is well known that 300 kW/m^3 is a practical design level for medium size power transformer [8]. As we can see from Fig. 2 which shows the power losses of this new DMR50B material as a function of temperature measured at different frequencies and different flux densities, at the measured temperature range, power losses of this material are almost less than 200 kW/m^3 in the frequency range of 100 kHz to 3 MHz, and under 3 MHz, 10 mT are only around 200 kW/m^3 at 100 °C and 150 kW/m^3 at 80 °C. This new material exhibits an extremely low core loss of around 20 kW/m^3 under the measurement condition of 700 kHz, 30 mT and 100 °C. Under 500 kHz to 1 MHz, the power loss at 80 °C is below 50 kW/m^3, and the lowest power loss is at 700 kHz and 30 mT, higher than that for DMR50, which is at 500 kHz and 50 mT [13]. So we can say that this material can be used in higher frequency up to 3 MHz with an extremely low power loss.

3.3. Relative importance and reducing the losses

To make this material suitable for frequencies above 1 MHz, P_h, P_e and P_r of this material have been improved by a total optimization of preparation conditions. As explained in Section 1 that P_e can be reduced by increasing the resistivity of the material. The resistivity inside grains and of grain boundaries in this material has been increased with the help of appropriate additives such as TiO_2, Nb_2O_5 and ZrO_2. Because the uniform grains are small in size (as will be seen later) and large grain resistivity, and inner grain eddy current losses due to micro-current inside grains do not show up at high frequencies, P_e is lowered. As P_h is also lowered by uniform microstructure with less voids and P_r is suppressed by using uniform fine grains, the total P_{CV} of this material at high frequencies is lowered.

As described above, the anisotropy compensation is such that the magnetocrystalline anisotropy constant K_1 as a function of temperature shows a minimum T_{min}. It is generally assumed that T_{min} corresponds to the temperature of the maximum permeability $T_{\mu max}$, because $T_{\mu max}$ is realized when K_1 becomes zero. As a consequence, hysteresis losses $P_h(T)$ shows a minimum, and the position of the P_h minimum T_{min} can be located at the intended working temperature [8]. It has been observed that if residual loss P_r becomes dominant at a high frequency and high temperature, T_{min} decreases far lower than that of the desired temperature when the frequency is increased, especially in the MHz range. Because P_r has become the main cause of the frequency dependence of the minimum loss temperature at high frequencies [7–9], P_r can create a frequency dependence for the minimum loss temperature [7], and this phenomenon also has been found in DMR50 material [13], whose chemical composition is supposed to be optimal for anisotropy compensation at about 80 °C. So DMR50 ferrite material should reach this minimum at that temperature if P_r is small, revealing that P_r of DMR50 material can be further lowered.

As can be seen from Fig. 2, P_{CV} drastically increases and T_{min} only changes a little around 80 °C with increasing frequency, being almost the same as the compensation point. At frequency below 1 MHz, T_{min} is around 70 °C; at frequency above 1 MHz, T_{min} is

Table 1
Important magnetic property for this new DMR50B material and comparison.

Property	Measurement conditions	DMR50B	DMR50	3F4
Initial permeability (μ_i)	25 °C; 10 kHz; <0.1 mT	1300	1400	900
Amplitude permeability (μ_a)	25 °C; 25 kHz; 200 mT	1990	2100	
	100 °C; 25 kHz; 200 mT	1950	2300	1700
Maximum induction (B_m, mT)	25 °C; 1194 A/m	510	490	410
	100 °C; 1194 A/m	430	400	350
Power losses (P_{CV}, kW/m^3)	100 °C; 500 kHz; 50 mT	80	60	
	100 °C; 700 kHz; 30 mT	20	70	
	100 °C; 1 MHz; 30 mT	70	160	130
	100 °C; 3 MHz; 10 mT	200	310	220
Curie temperature (°C)		290	250	220
Resistivity (ρ, Ω m)		8	8	10
Density (d, kg/m^3)		4.7×10^3	4.7×10^3	4.7×10^3

around 80 °C. Obviously, T_{min} is usually located at around 80 °C for all the frequencies observed. As a result, we can conclude that P_r of this DMR50B material is really suppressed at high frequencies [7], resulting in an extremely low loss material due to the homogeneity of the microstructure.

It has been found that P_r will increase with relative permeability μ_r [7], which can be lowered by fine grains. Since P_r becomes dominant at high frequency, lowered μ_r will reduce P_r in the MHz range. We can see from Table 1 that μ_a is lower for DMR50B than that for DMR50 even at a high temperature, and that P_r is reduced because of its smaller grain size than that of DMR50 (as will be seen later).

Just as described earlier, the constitution of the total power loss P_{CV} depends on frequency and on induction level. It has been found that the power loss (P_{CV}) can also be expressed as a function of frequency (f) and magnetic flux density (B):

$$P_{CV} = kB^x f^y \tag{3}$$

where x and y are called Steinmetz coefficients [5,6,23]. For typical Mn–Zn ferrites intended for power applications, the Steinmetz coefficient (x) lies between 2 and 3, and y is about 1.3 up to 100 kHz [5,6,14]. It has been found that, the power loss increased linearly with increasing frequency ($y \approx 1.25$) at low frequency, and at high frequency, deviated from the linearity, where the coefficient of frequency (y) was 2.87 at 100 °C and 25 mT [5]. Strictly speaking, this equation is valid over different limited ranges, and may be used effectively over these limited frequency ranges, because the main contribution to P_{CV} is different at different frequency range, as can be seen in Eq. (1) and the later discussion. Basically speaking, the power loss property of DMR50B material is the same as DMR50, including P_{CV}–T, P_{CV}–B and P_{CV}–f, but DMR50B has lower power loss than that of DMR50.

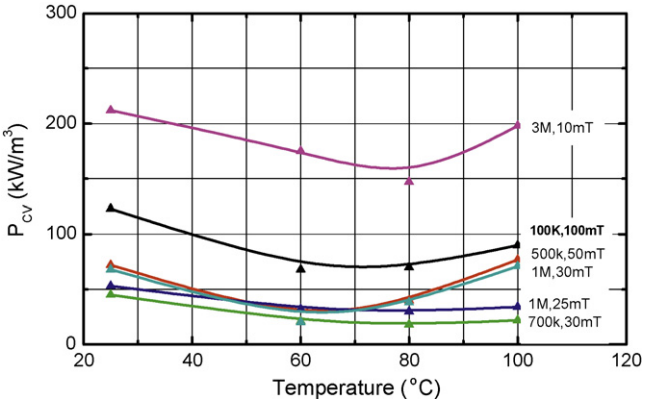

Fig. 2. Power losses for various measuring conditions as a function of temperature.

3.4. P_{CV} vs B

Fig. 3 shows the power losses of this material as a function of B measured at various frequencies. P_{CV} of this material increases with increasing B and follows the relation described in Eq. (3) in different B ranges, where we can see the measuring frequency dependence of the Steinmetz coefficient (x). It is well known that at lower frequencies, P_{CV} is mostly ascribed to P_h which is proportional to the third power of B, but at high frequency, P_e becomes dominant and is proportional to the square term of B, just as expressed in Eq. (1). As can be seen from Fig. 3, at the beginning, P_{CV} increases linearly with B, but when B becomes bigger, the first deviations from the linearity can be seen, indicating that the power loss mechanism has changed, especially at high frequencies. At the frequencies above 500 kHz, when B is large enough, these second deviations can be clearly seen, which are caused by the increase of P_r. Careful analysis shows that P_{CV} dependence on B at various frequencies is in good agreement with the proposed relation expressed in Eq. (3) in different B ranges, and will be published elsewhere.

3.5. P_{CV} vs frequencies

Fig. 4 shows the power losses plotted as a function of frequency at various magnetic flux densities. A similar power loss behavior versus frequency is observed. P_{CV} of this material increases with increasing frequency and follows the relation described in Eq. (3) at different frequency ranges, from which we can deduce the measuring B dependence of the Steinmetz coefficient (y). It can be clearly seen that, when B is small, the power loss increases linearly in the low-frequency range and then deviates from the linearity at above

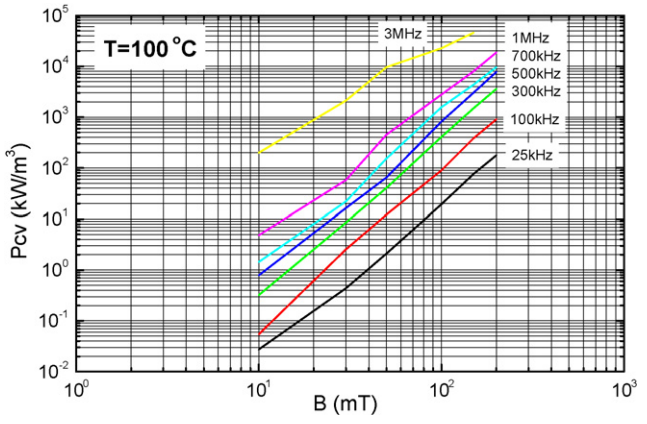

Fig. 3. Power losses for various frequencies as a function of magnetic flux density at 100 °C.

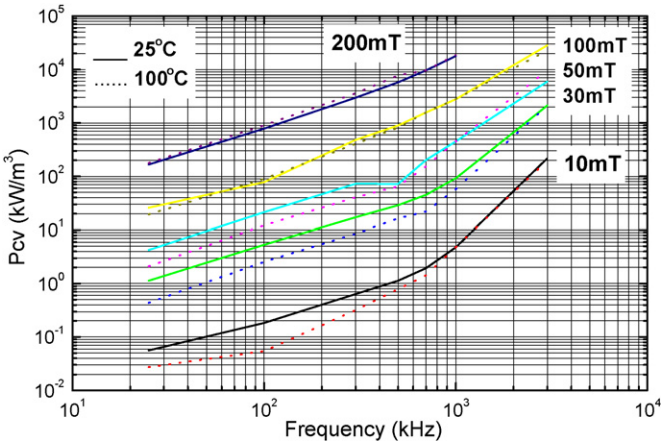

Fig. 4. Power losses for various magnetic flux densities as a function of frequency at 25 and 100 °C.

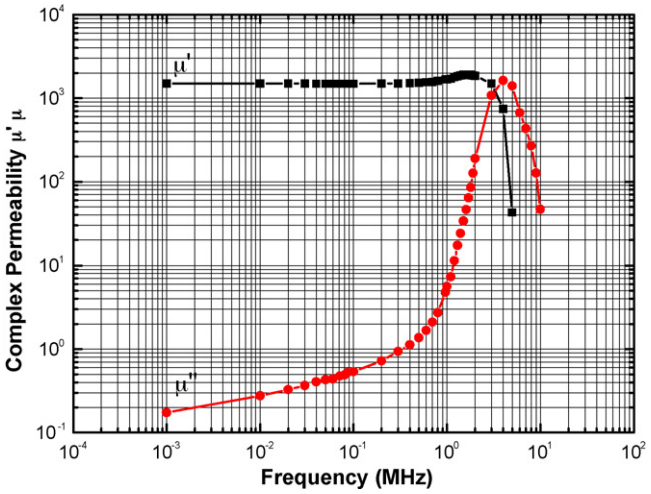

Fig. 5. Frequency dependence of complex permeability.

about 100 kHz, and then again deviates at above 500–700 kHz. These deviations from the linearity indicate that the constitution of total loss P_{CV} is different at different frequency ranges, just as discussed above in Fig. 3. As we have seen, P_h is the major part of P_{CV} at frequencies below 100 kHz ($P_h \propto f$), and then P_e becomes important at frequencies higher than 100 kHz ($P_e \propto f^2$) according to Eq. (1), but when the ferrite is used at frequencies above 500–700 kHz, P_r becomes dominant, just as we can see from Fig. 4 that at this high frequency range, P_r increases rapidly, resulting in a large deviation, being the same as discussed above in Fig. 3. This can also be clearly seen in Fig. 2, which shows that the P_{CV} at 3 MHz increases a lot compared to that at 1 MHz. This is also in good agreement with the proposed relation expressed in Eq. (3) in different frequency ranges. Careful analysis of these deviations will also be published elsewhere.

We can also see from Fig. 4, when B is large enough, such as 200 mT, these deviations can obviously be observed. The same situation can also be found in DRM50 material [13]. It is noted that [24], when the ferrite is driven at high flux level at high frequencies, the conductivity is highly non-linear, which is consistent with inter-granular charge tunneling between neighboring ferrite grains through the thin insulating films (grain boundaries). When the flux density levels used are higher enough, they may give rise to large induced electric fields at the grain boundaries to cause tunneling. Perhaps this non-linear increase behavior of conductivity can explain this observed B dependence of the power loss at high frequencies.

As can be seen from Fig. 4, the slopes of the lower frequency portion of the 10 mT curve and the central portion of the 50 mT curve are lower than 1, which is unphysical. This phenomenon also exists in DMR50 material [13]. At the cross-point where the major part of P_{CV} will change, such as change from P_h to P_e, and from P_e to P_r, there will be an abnormal increase in P_{CV}. Possibly this abnormal increase together with the non-linear increasing behavior of the power loss over B can explain this unphysical behavior. This abnormal increase can also cause big errors in measuring the power loss.

We can also see from Figs. 3 and 4 that the slopes of P_{CV}–B and P_{CV}–f curve are smaller compared to those of old DMR50 material in different corresponding ranges, indicating that the P_{CV} of DMR50B has been improved in high frequencies. Detailed analysis will be published elsewhere.

3.6. Magnetic spectrum

Fig. 5 shows the magnetic spectrum of this material. We can see that its cutoff frequency, where μ' falls to half its original value or μ'' gets its maximum value, is as high as about 4 MHz, almost the same as DMR50 material [13]. These two materials can all be used to frequency above 3 MHz, though traditionally it is believed that MnZn soft ferrite can only be used to frequency up to 1 MHz, again we find that this is not always the case. This is because of its fine grains, as will be seen later.

Snoek pointed out that at MHz frequencies a ferromagnetic resonance occurs if the frequency of the applied field equals the precession frequency of the spins in the internal field, f_r, and that this resonance dominates the ferrite dissipation in the MHz range [25]. Magnetic rotational resonance occurs when the driving frequency is in resonance with the natural frequency at which the magnetization rotates, and then there is a large peak in power absorption. The resonance frequency is given by Snoek's law [8,9,25]:

$$f_r = \frac{\gamma B_m}{3\pi\mu_0(\mu_r - 1)} \tag{4}$$

where B_m is the maximum induction, μ_r is the low-frequency rotational contribution to the initial magnetic permeability and γ is the gyromagnetic ratio. Snoek derived under the assumption that the initial permeability of the ferrite is due to rotation of spins. As domain wall resonance is usually of less relevance at frequencies important for power ferrites [8], assuming a dominating rotational character for the magnetic permeability, we can calculate f_r value according to Snoek's law. Assuming $\mu_r = 1990$ and applying $B_m = 510$ mT from Table 1, Eq. (4) yields $f_r \approx 4.8$ MHz, a little higher than that of DMR50, which is 4.4 MHz [13]. As can be seen from Eq. (4), μ_r of this material is lowered by small grains compared with conventional power ferrites, so f_r is increased. Snoek demonstrated that an increase in permeability could increase the operating frequency of a ferrite only when there is a simultaneous increase in B_m [25]. Because its B_m is higher and μ_r is smaller than that of DMR50, leading to a higher f_r according to Eq. (4). The result turns out to be quite reasonably in accord with the experimental data, indicating that the resonances that occurred in power ferrites at this operation frequency range are truly rotational resonances, and that the rotational component of the magnetic permeability is clearly dominant because domain walls can no longer follow the alternating magnetic field [8], which was similarly found in DMR50 material [13].

In addition, as we can see that, the permeability of 1990 assumed above is the permeability of the polycrystalline system, but the law of Snoek is derived and holds for monocrystalline materials. Among the most basic questions addressed specifically to ceramic materials is how the magnetic permeability depends on grain size,

grain boundary structure, etc. [26]. As far as their influence on the permeability is concerned, the present state of knowledge can be summarized as follows: the permeability in ferrites is predominantly rotational in character, particularly for the smaller grain size [27]. Proceeding to small grains eventually leads to the monodomain state where no magnetic domain walls can exist inside single grains. In this case domain walls can only exist in grain boundary regions, as will be discussed later.

It has been described by the non-magnetic grain boundary model [28,29] that Snoek's law will translate to polycrystalline materials in case of rotational permeability, and this model also predicts that polycrystalline systems will have a higher resonance frequency than monocrystalline forms with identical composition despite the fact that the size of the thickness of the non-magnetic grain boundary has to be adjusted to the experiments [17,28,29]. As domain wall motion model [30], which is considered to account for the dependence of the initial permeability μ_i on grain size in polycrystalline ferrites, is less favourable in smaller grains, it is recognized that the non-magnetic grain boundary model [28,29] is able to account not only for the observed grain size dependence of μ_i, but also for the observed frequency dependence of the full complex permeability (agreement with Snoek's law). The essential feature of this model shows that the polycrystalline ferrite consists of a matrix of crystalline ferrite grains, having an intrinsic permeability (in fact the permeability of a single crystal of the same composition), surrounded by thin, non-magnetic grain boundaries with unit permeability. Additionally, a first principles model for the grain boundary developed in Ref. [26], which is responsible for the distinct dependence of permeability of ceramic soft magnetic ferrites on grain size in a quantitative fashion, also gets the same results without any adjustable parameter while maintaining Snoek's limit. This model involves boundary conditions for the spin system at the exchange-decoupled interfaces of adjacent grains and an inhomogeneous free energy density which brings the domain wall width as a natural length scale into the problem. This scale will precisely determine the grain size beyond which the permeability significantly starts to decrease. So Snoek's law remains valid when the initial permeability of a ferrite is decreased by reducing its grain size, i.e., fine-grained materials display a higher resonance frequency and can therefore be used to higher frequencies [9,28,29].

3.7. DC-bias properties

This material also has very good DC-bias properties, as shown in Fig. 6. The incremental permeability μ_Δ of this material almost remains constant until its DC-bias magnetic field H_{DC} is as high as 100 A/m (which is only 30 A/m for DMR50 material), where it starts

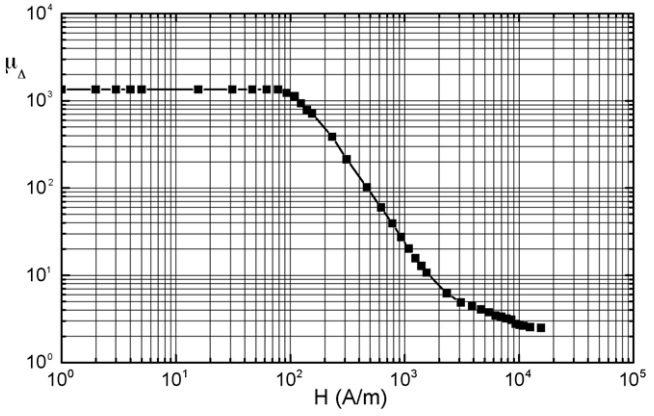

Fig. 6. Incremental permeability as a function of magnetic field *H*.

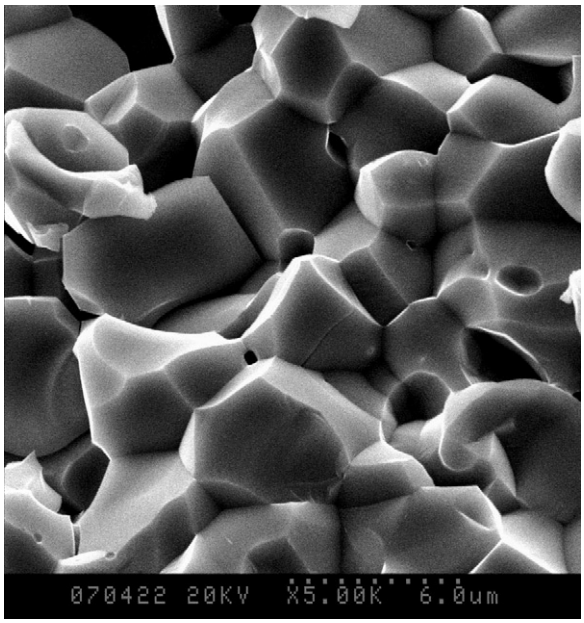

Fig. 7. Typical SEM image of the microstructure of this DMR50B material.

to decrease. We have also measured the DC magnetic properties of this material, see Table 1. Note that in Table 1, B_m of this material is about 430 mT at 100 °C when measured at 1194 A/m, and its Curie temperature is as high as 290 °C. Because of its higher B_m compared with that of DMR50, its DC-Bias property is also improved a lot. All these show that this material has very good physical properties, and can be used as a high DC-bias power material at frequency higher than 3 MHz.

3.8. SEM

As far as we know, the magnetic property of a magnetic material is closely related to its microstructure. We have investigated the microstructure of this ferrite material using SEM, as shown in Fig. 7. As can be seen in SEM, compared with DMR50 material, there exists less voids, the inner part of the grains is homogeneous and free of impurities, pores and other defects, grain size is relatively uniform, and the voids can rarely be seen in the grains and are only distributed in grain boundary regions, suggesting that this material has been optimized, and so its magnetic properties are improved. EDX analysis shows that the chemical composition is just the same as we have chosen.

It has a more uniform grain growth, the average grain size is about 2.40 μm, smaller than that of DMR50, which reduces the P_r in high frequencies, and also makes the high peak of complex permeability [9–11]. Intragranular domain wall movement is a prime contribution to the AC-hysteresis (in particular, at frequencies around 1 MHz), and this hysteresis is eliminated in fine-grained, single domain ferrites [9–12]. If the grain size is smaller than the single domain size, the domain wall can only exist in the grain boundary regions. For Mn–Zn ferrite, the transition in the intragranular domain structure from the single domain to the multiple domain state occurs at the grain size 3.8 ± 0.7 μm [9–11], it is also found that there is a drastic increase in P_r at the grain size around 4 μm [12], suggesting that P_r due to the domain wall resonance should be taken into account at the grain size greater than single domain dimension. This means when the grain size is greater than the single domain dimension, P_r due to domain wall relaxation process as well as the rotational resonance process should be taken into account. This material has small, uniformly sized and densely dis-

tributed crystalline grains and less voids, which indicates that there exists less exaggerated grain growth and thus better microstructure homogeneity than DMR50, resulting in higher B_m, and thus improved DC-bias properties. So, as a Mn–Zn ferrite that can work at frequencies higher than 3 MHz because of its fine grain size, the lowest power loss values are derived from the more regular and homogeneous microstructures.

4. Conclusions

Based on our previous study of DMR50, which reveals that its P_r can be further lowered, and also the need to improve the DC-bias property of DMR50, Mn–Zn power ferrite DMR50B with an extremely lower loss used at higher frequencies was developed employing a conventional ceramic powder processing technique. SEM study shows that the average grain size is 2.40 μm, smaller than that needed for the single domain dimension, and XRD analysis shows that the grain is well crystallized. As a result, power loss of this material is less than 200 kW/m^3 in the frequency range of 100 kHz to 3 MHz at the measured flux density levels over a wide temperature range, and is only around 20 kW/m^3 under 700 kHz, 30 mT and 100 °C due to its desired microstructures. In addition, its B_m is about 430 mT at 100 °C when measured at 1194 A/m, and it also has attractive DC-bias property, its DC-bias magnetic field H_{DC} is 100 A/m. Furthermore, the cutoff frequency of this material is as high as 4 MHz, which means that this material can be used at frequency higher than 3 MHz. Its better magnetic properties are derived from densely sintered ferrite with the more regular and homogeneous microstructure.

Acknowledgements

The authors are very much thankful to Dr. Wenhong Sun and Liping Wang of Zhejiang Jixiang Industry Co. Ltd. for helpfull discussions and also English writing. This work is supported by 151 Fund, Analysis and Test Fund A (no. 04089), and also Fund for Key Nano-technical problem (no. 2005C11042) of Zhejiang province of P.R. of China.

References

[1] C. Beatrice, O. Bottauscio, M. Chiampi, F. Fiorillo, A. Manzin, J. Magn. Magn. Mater. 304 (2006) e743–e745.
[2] G. Ott, J. Wrba, R. Lucke, J. Magn. Magn. Mater. 254–255 (2003) 535–537.
[3] S. Otobe, Y. Yachi, T. Hashimoto, T. Tanimori, T. Shigenaga, H. Takei, K. Hontani, IEEE Trans. Magn. 35 (5) (1999) 3409–3411.
[4] S. Yamada, E. Otsuki, J. Magn. Soc. Jpn. 19 (1995) 421–424.
[5] W.H. Jeong, B.M. Song, Y.H. Han, Jpn. J. Appl. Phys. 41 (2002) 2912–2915.
[6] E.C. Snelling, Soft Ferrites, 2nd ed., Butterworths, London, 1988, p. 90.
[7] O. Inoue, N. Matsutani, K. Kugimiya, IEEE Trans. Magn. 29 (6) (1993) 3532–3534.
[8] D. Stoppels, J. Magn. Magn. Mater. 160 (1996) 323–328.
[9] P.J. Van der Zaag, J. Magn. Magn. Mater. 196–197 (1999) 315–319.
[10] P.J. van der Zaag, P.J. van der Valk, M.Th. Rekveldt, Appl. Phys. Lett. 69 (1996) 2927–2929.
[11] P.J. van der Zaag, J.J.M. Ruigrok, A. Noordermeer, M.H.W.M. van Delden, P.T. Por, M.Th. Rekveldt, D.M. Donnet, J.N. Chapman, J. Appl. Phys. 74 (1993) 4085–4095.
[12] V. Zaspalis, V. Tsakaloudi, E. Papazoglou, M. Kolenbrander, R. Guenther, P. van der Valk, J. Electroceram. 13 (2004) 585–591.
[13] Y.P. Liu, S.J. He, J. Magn. Magn. Mater. 320 (23) (2008) 3318–3322.
[14] K. Sun, Z.W. Lan, Z. Yu, L.Z. Li, X.L. Nie, Z.Y. Xu, J. Alloys Compd. 468 (2009) 315–320.
[15] E. Melagiriyappa, H.S. Jayanna, J. Alloys Compd. 482 (2009) 147–150.
[16] M. Gu, G. Liu, J. Alloys Compd. 475 (2009) 356–360.
[17] L. Li, Z. Lan, Z. Yu, K. Sun, Z. Xu, J. Alloys Compd. 476 (2009) 755–759.
[18] C.F. Zhang, X.C. Zhong, H.Y. Yu, Z.W. Liu, D.C. Zeng, Physica B 404 (2009) 2327–2331.
[19] W. Wang, J. Wang, J. Alloys Compd. 463 (1–2) (2008) 112–118.
[20] M. Mozaffari, F. Ebrahimi, S. Daneshfozon, J. Amighian, J. Alloys Compd. 449 (1–2) (2008) 65–67.
[21] M.J. Nasr Isfahani, M. Myndyk, V. Šepelák, J. Amighian, J. Alloys Compd. 470 (1–2) (2009) 434–437.
[22] K. Praveena, K. Sadhana, S. Bharadwaj, S.R. Murthy, J. Magn. Magn. Mater. 321 (2009) 2433–2437.
[23] E.C. Snelling, A.D. Giles, Ferrites for Inductors and Transformers, Research Studies Press, 1983, p. 136.
[24] W.A. Roshen, J. Magn. Magn. Mater. 312 (2007) 245–251.
[25] J.L. Snoek, Nature 160 (1947) 90–190.
[26] J. Pankert, J. Magn. Magn. Mater. 138 (1994) 45–51.
[27] E.G. Visser, J.J. Roelofsma, G.J.M. Aaftink, Proc. 5th Int. Ferrites Conf. Bombay, 1989, pp. 605–609.
[28] M.T. Johnson, E.G. Visser, IEEE Trans. Magn. 26 (5) (1990) 1987–1989.
[29] E.G. Visser, M.T. Johnson, J. Magn. Magn. Mater. 101 (1–3) (1991) 143–147.
[30] A. Globus, J. Phys. Suppl. C1 (1977) 1–15 (Proc. ICF3).